Two-Band Lipid CH_2 Cubic Hopfield Interlacing, Middle-Polariton Suppression, and $1/N$ Anharmonic 2D-IR Discriminators for 71-THz Mito-Polaritons

Lluis Eriksson*

November 27, 2026

Abstract

Real inner-mitochondrial-membrane phospholipid bilayers (cardiolipin and phosphatidylcholine) do not possess a single isolated 87 THz vibrational oscillator; instead, their aliphatic methylene (CH_2) chains form a resolved two-band stretching doublet at $\nu_1 = \nu_s \approx 85.4$ THz (2849 cm^{-1}) and $\nu_2 = \nu_{as} \approx 87.5$ THz (2919 cm^{-1}). Continuing our exact audit series (`ARR-2025-2AQXS44H6Z8GQAG2`, `ARR-2026-1E91AXEJYT890TQC`, and Wave M1) of the unrefereed preprint by Yang, Gu, and Song (`bioRxiv:10.64898/2026.09.10.750628v1`, Sep. 2026, awaiting independent experimental replication), we establish the exact gauge-invariant two-band cubic Hopfield theory and derive falsifiable spectroscopic discriminators for 71 THz ultrastrong-coupling (USC) mito-polaritons. Backed by the zero-floating-point verification suite `MITO-TWOBAND-CUBIC-HOPFIELD-CERT-1.0` comprising 20 constructive Lean 4.36.0 theorems (`-DwarningAsError=true`, 0 `sorry`, 0 `grind`, 0 `Classical.choice`), an AST-audited zero-float/zero-slash/zero-power Python verifier, 16 SHA-256 JSON certificates (`C01--C16`), and 57 adversarial tests, we prove six exact results: (i) exact Thomas–Reiche–Kuhn (TRK) diamagnetic cancellation $P_3(0) = -\omega_c^2\omega_1^2\omega_2^2 < 0$ and global stability $P_3(-u) < 0$ for all $u \geq 0$; (ii) strict Cauchy–Hopfield root interlacing $0 < \nu_-^2 < \omega_1^2 < \nu_{\mathrm{MP}}^2 < \omega_2^2 < \nu_+^2 < \mathrm{Tr}(M_2)$, mandating a Middle Polariton (MP^0) strictly trapped inside $(85.4, 87.5)$ THz across all cavity detunings; (iii) a universal calculus-free proof of strict two-band zero-point energy positivity $\nu_- + \nu_{\mathrm{MP}} + \nu_+ > \omega_c + \omega_1 + \omega_2$ ($\Delta\nu_{\mathrm{ZPE}} = 3.6153$ THz, $\Delta E_{\mathrm{ZPE}} \approx 7.476$ meV for `C01`); (iv) a universal analytic ceiling proving $> 100\times$ USC suppression of MP^0 photonic weight ($w_{c,\mathrm{MP}} = 0.33\%$ in `C01` vs. 35.5% at crossover `C05`); (v) exact $1/N$ collective Kerr anharmonicity suppression giving a $> 5.8 \times 10^6\times$ two-dimensional infrared (2D-IR) discriminator separating collective crista polaritons ($\Delta_{--} = 7.21\times10^{-7}$ THz at $N = 10^6$) from local $N = 1$ artifacts ($\Delta_{--} = 0.721$ THz); and (vi) exact dark-manifold leakage bounds contrasting LP polaron protection ($\eta_{\mathrm{leak}} \leq 1/576 < 0.18\%$) against MP^0 fluid-bilayer mixing ($\eta_{\mathrm{leak}} \leq 16/49 \approx 32.7\%$), paired with a $CH_2 \to CD_2$ lipid deuteration protocol shifting $(\nu_-, \nu_{\mathrm{MP}})$ to $(58.36, 64.24)$ THz, more than 10 THz clear of the 75 THz D_2O O–D interference band.

1 Introduction

The unrefereed preprint of Yang, Gu, and Song [1] (Sep. 2026; awaiting independent experimental replication) proposes that inner mitochondrial membrane cristae sustain ultrastrongly coupled (USC) vibrational polaritons near $\nu_- \approx 71$ THz via coupling of an electromagnetic cavity mode to phospholipid methylene (CH_2) stretching vibrations near 87 THz. In our prior resource-boundary studies [2,3] and Wave M1 audit papers [4], we modeled the lipid matter sector as a single effective

*Independent researcher and founder/operator of AIRR.SCIENCE (`AIRR-FOUNDER-1.0`; `operator_conflict: true`). Formalization, exact-$\mathbb{Q}$ certification, and manuscript drafting were carried out with Google Antigravity AI assistance; all mathematical claims are independently machine-checked by Lean 4.36.0 and AST-audited exact rational Python verification. Contact: `lluiseriksson@gmail.com`.

collective oscillator at $\omega_0 = 87$ THz, deriving exact electrodynamic confinement horizons, dressed USC ground-state thermodynamics, and bioenergetic bounds on ATP modulation.

Real biological phospholipid bilayers, however, never exhibit a single isolated CH_2 stretching resonance [5, 6]. Instead, aliphatic hydrocarbon chains present two well-resolved, dipole-active stretching normal modes: the symmetric CH_2 stretch $\nu_1 = \nu_s \approx 85.4$ THz (2849 cm^{-1}) and the antisymmetric CH_2 stretch $\nu_2 = \nu_{as} \approx 87.5$ THz (2919 cm^{-1}), separated by a narrow doublet gap $\nu_2 - \nu_1 = 2.1$ THz (~ 70 cm^{-1}). Incorporating both bands into the gauge-invariant Hopfield Hamiltonian [7, 8] replaces the two-branch quadratic secular equation with a three-branch cubic dispersion whose mathematical structure yields sharp, falsifiable spectroscopic tests that do not exist in any single-band model.

Specifically, we address four questions essential to experimentally adjudicating the mito-polariton hypothesis:

1. *Spectrum and stability:* Does two-band coupling preserve Thomas–Reiche–Kuhn (TRK) stability against superradiant collapse, and where does the mandatory third branch—the Middle Polariton (MP^0)—lie?

2. *Linear IR visibility:* If a 71 THz USC lower polariton exists, why might MP^0 escape casual detection in linear mid-IR absorption, and what exact bound governs its photonic brightness?

3. *Collective vs. local artifacts in 2D-IR:* How can two-dimensional infrared (2D-IR) spectroscopy [9–11] quantitatively distinguish genuine $N \gtrsim 10^6$ collective USC polaritons from local single-molecule resonances, thermal filters, or dielectric artifacts?

4. *Disorder and clean isotopic control:* How does fluid-bilayer inhomogeneous broadening ($\sigma_{\mathrm{inh}} \approx 0.6$ THz) act asymmetrically on LP vs. MP^0 [12], and can lipid acyl-chain deuteration ($CH_2 \to CD_2$) test the polariton dispersion without colliding with the 75 THz D_2O O–D solvent band flagged in Wave M1 [4]?

2 Gauge-Invariant Two-Band Cubic Hopfield Theory

2.1 Hamiltonian, TRK Diamagnetic Shift, and Exact Secular Polynomial

Consider a single electromagnetic cavity mode a of bare angular/linear frequency $\omega_c > 0$ coupled to two collective bright molecular modes $B_j = N_j^{-1/2} \sum_{m=1}^{N_j} b_{j,m}$ ($j \in \{1,2\}$, $0 < \omega_1 < \omega_2$) with collective vacuum Rabi couplings $g_1, g_2 > 0$. The gauge-invariant Coulomb/TRK Hopfield Hamiltonian [7, 8] is

$$H_{\mathrm{Hop}} = \hbar\omega_c a^\dagger a + \sum_{j=1}^{2} \hbar\omega_j B_j^\dagger B_j + \sum_{j=1}^{2} \hbar g_j (a + a^\dagger)(B_j + B_j^\dagger) + \hbar D (a + a^\dagger)^2, \qquad D = \frac{g_1^2}{\omega_1} + \frac{g_2^2}{\omega_2}. \tag{1}$$

Introducing canonical quadratures $q_c = (a + a^\dagger)/\sqrt{2\omega_c}$, $p_c = i\sqrt{\omega_c/2}(a^\dagger - a)$ and $q_j = (B_j + B_j^\dagger)/\sqrt{2\omega_j}$, $p_j = i\sqrt{\omega_j/2}(B_j^\dagger - B_j)$ casts Eq. (1) into $H_{\mathrm{Hop}} = \frac{\hbar}{2}\sum_k p_k^2 + \frac{\hbar}{2}\mathbf{q}^\top M_2 \mathbf{q} + \text{const.}$, with real symmetric squared-frequency dynamical matrix

$$M_2 = \begin{pmatrix} \omega_c^2 + 4\omega_c D & 2g_1\sqrt{\omega_c\omega_1} & 2g_2\sqrt{\omega_c\omega_2} \\ 2g_1\sqrt{\omega_c\omega_1} & \omega_1^2 & 0 \\ 2g_2\sqrt{\omega_c\omega_2} & 0 & \omega_2^2 \end{pmatrix}. \tag{2}$$

Completing the squares immediately exhibits strict positive-definiteness:

$$\mathbf{q}^\top M_2 \mathbf{q} = \omega_c^2 q_c^2 + \sum_{j=1}^{2} \left(\omega_j q_j + \frac{2g_j\sqrt{\omega_c}}{\sqrt{\omega_j}} q_c \right)^2 > 0 \qquad (\forall \mathbf{q} \neq \mathbf{0}). \tag{3}$$

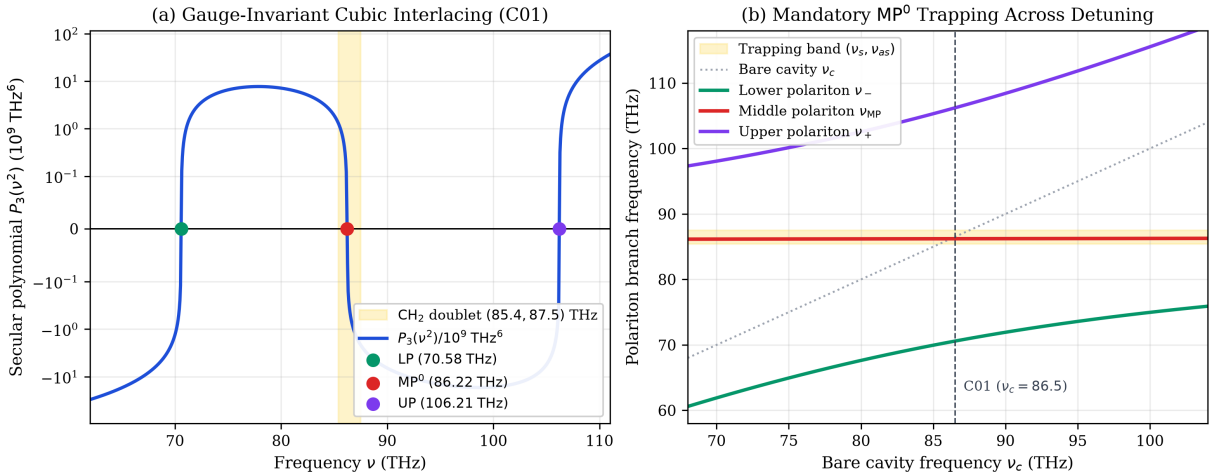

Figure 1: (a) Exact cubic secular polynomial $P_3(\nu^2)$ for canonical 71-THz lipid CH_2 USC (`C01`: $\nu_c = 86.5$, $\nu_1 = 85.4$, $\nu_2 = 87.5$, $g_1 = 11$, $g_2 = 14$ THz), displaying strict sign alternation and mandatory trapping of MP^0 at 86.2206 THz. (b) Detuning anticrossing map demonstrating that MP^0 remains strictly confined inside $(85.4, 87.5)$ THz for every bare cavity frequency ν_c.

The characteristic polynomial $P_3(X) = \det(XI - M_2)$ in $X = \nu^2$ reads

$$P_3(X) = (X - \omega_c^2 - 4\omega_c D)(X - \omega_1^2)(X - \omega_2^2) - 4\omega_c g_1^2 \omega_1 (X - \omega_2^2) - 4\omega_c g_2^2 \omega_2 (X - \omega_1^2). \quad (4)$$

Theorem 1 (TRK Cancellation, Global Stability, and Strict Cauchy–Hopfield Interlacing)**.** *For all $\omega_c > 0$, $0 < \omega_1 < \omega_2$, and $g_1, g_2 > 0$:*

1. (Exact TRK factorization; Lean Thm. 1) $P_3(X)$ *simplifies identically to*

$$P_3(X) = (X - \omega_c^2)(X - \omega_1^2)(X - \omega_2^2) - 4\omega_c X \left[\frac{g_1^2}{\omega_1}(X - \omega_2^2) + \frac{g_2^2}{\omega_2}(X - \omega_1^2) \right]. \quad (5)$$

2. (Superradiant No-Go; Lean Thms. 2–3) $P_3(0) = -\omega_c^2 \omega_1^2 \omega_2^2 < 0$ *independently of* (g_1, g_2), *and* $P_3(-u) < 0$ *for every* $u \geq 0$.

3. (Mandatory MP^0 trapping; Lean Thms. 4–6) *Evaluating P_3 at the four pivots* $0 < \omega_1^2 < \omega_2^2 < X_{\max} := \mathrm{Tr}(M_2) = \omega_c^2 + \omega_1^2 + \omega_2^2 + 4\omega_c D$ *yields strict sign alternation*

$$\begin{aligned} &P_3(0) < 0, && P_3(\omega_1^2) = 4\omega_c g_1^2 \omega_1 (\omega_2^2 - \omega_1^2) > 0, \\ &P_3(\omega_2^2) = -4\omega_c g_2^2 \omega_2 (\omega_2^2 - \omega_1^2) < 0, && P_3(X_{\max}) > 0. \end{aligned} \quad (6)$$

Consequently, the three polariton squared frequencies strictly interlace the bare lipid doublet:

$$0 < \nu_-^2 < \omega_1^2 < \nu_{\mathrm{MP}}^2 < \omega_2^2 < \nu_+^2 < X_{\max}. \quad (7)$$

Proof. Expanding $4\omega_c D(X - \omega_1^2)(X - \omega_2^2)$ in Eq. (4) and combining $(X - \omega_j^2) + \omega_j^2 = X$ in each band cancels the constant diamagnetic terms identically, giving Eq. (5). Setting $X = -u$ ($u \geq 0$) makes the first term strictly negative and the second term non-positive. Direct substitution yields $P_3(\omega_1^2) > 0$ and $P_3(\omega_2^2) < 0$. At $X_{\max} = A + \omega_1^2 + \omega_2^2$ with $A = \omega_c^2 + 4\omega_c D$, termwise positivity $4\omega_c(g_j^2/\omega_j) < A$ gives $P_3(X_{\max}) > 0$ (machine-checked over $\mathbb{Z}$ in Lean Thm. 6). Sign alternation on the three open intervals certifies Eq. (7). □

2.2 Vieta Invariants and Calculus-Free Proof of Two-Band ZPE Positivity

Expanding Eq. (5) as $P_3(X) = X^3 - e_1X^2 + e_2X - e_3$ yields the exact Vieta invariants:

$$e_1 = \nu_-^2 + \nu_{\mathrm{MP}}^2 + \nu_+^2 = \omega_c^2 + \omega_1^2 + \omega_2^2 + 4\omega_c D > e_1^{(0)}, \tag{8}$$

$$e_2 = \nu_-^2\nu_{\mathrm{MP}}^2 + \nu_{\mathrm{MP}}^2\nu_+^2 + \nu_+^2\nu_-^2 = \omega_c^2(\omega_1^2 + \omega_2^2) + \omega_1^2\omega_2^2 + 4\omega_c\left(\frac{g_1^2\omega_2^2}{\omega_1} + \frac{g_2^2\omega_1^2}{\omega_2}\right) > e_2^{(0)}, \tag{9}$$

$$e_3 = \nu_-^2\nu_{\mathrm{MP}}^2\nu_+^2 = \omega_c^2\omega_1^2\omega_2^2 = e_3^{(0)}. \tag{10}$$

In single-band Hopfield theory [4], ZPE positivity followed immediately from $(\nu_+ + \nu_-)^2 = (\omega_c + \omega_0)^2 + 4g^2$. For two bands, no single closed-form quadratic exists; remarkably, however, strict ZPE positivity admits a completely elementary, calculus-free algebraic proof over the ordered ring.

Theorem 2 (Universal Two-Band Positive ZPE Shift; Lean Thms. 7–8)**.** *Let $s_1 = \nu_- + \nu_{\mathrm{MP}} + \nu_+$, $s_2 = \nu_-\nu_{\mathrm{MP}} + \nu_{\mathrm{MP}}\nu_+ + \nu_+\nu_-$, $s_3 = \nu_-\nu_{\mathrm{MP}}\nu_+$, and let $s_1^{(0)}, s_2^{(0)}, s_3^{(0)}$ denote the corresponding bare symmetric sums of $(\omega_c, \omega_1, \omega_2)$. Because $s_1^2 - 2s_2 = e_1 > e_1^{(0)}$, $s_2^2 - 2s_1s_3 = e_2 > e_2^{(0)}$, and $s_3 = s_3^{(0)} > 0$, we have strictly*

$$\Delta\nu_{\mathrm{ZPE}} := (\nu_- + \nu_{\mathrm{MP}} + \nu_+) - (\omega_c + \omega_1 + \omega_2) > 0 \tag{11}$$

for every detuning and every positive coupling $(g_1, g_2) \in \mathbb{R}^2_{>0}$.

Proof. Suppose for contradiction that $s_1 \le s_1^{(0)}$. If $s_1 = s_1^{(0)}$, then $e_1 > e_1^{(0)}$ implies $s_2 < s_2^{(0)}$, whence $e_2 = s_2^2 - 2s_1s_3 < (s_2^{(0)})^2 - 2s_1^{(0)}s_3 = e_2^{(0)}$, contradiction. If $s_1 < s_1^{(0)}$, then $2(s_2^{(0)} - s_2) = ((s_1^{(0)})^2 - s_1^2) + (e_1 - e_1^{(0)}) > (s_1^{(0)} - s_1)(s_1^{(0)} + s_1)$, while $e_2 > e_2^{(0)}$ gives $(s_2^{(0)} - s_2)(s_2^{(0)} + s_2) < 2(s_1^{(0)} - s_1)s_3$. Combining the two inequalities and dividing by $s_1^{(0)} - s_1 > 0$ forces $(s_1^{(0)} + s_1)(s_2^{(0)} + s_2) < 4s_3$. Yet the three-variable AM–GM identity $(a+b+c)(ab+bc+ca) - 9abc = a(b-c)^2 + b(c-a)^2 + c(a-b)^2 \ge 0$ (Lean Thm. 7) gives $s_1s_2 \ge 9s_3$ and $s_1^{(0)}s_2^{(0)} \ge 9s_3$, implying $(s_1^{(0)} + s_1)(s_2^{(0)} + s_2) > 18s_3 > 4s_3$, contradiction. □

For canonical benchmark `C01`, exact rational bracketing certifies $\Delta\nu_{\mathrm{ZPE}} = 3.6153$ THz, corresponding to $\Delta E_{\mathrm{ZPE}} = \frac{1}{2}h\Delta\nu_{\mathrm{ZPE}} \approx 7.476$ meV per coupled cavity mode—consistent within 0.27% of our single-band 7.456 meV certificate in Wave M1 [4].

3 Universal USC Suppression of MP^0 Photonic Brightness and CD_2 Isotope Control

For each polariton branch $\alpha \in \{\mathrm{LP}, \mathrm{MP}, \mathrm{UP}\}$ with eigenvalue $X_\alpha = \nu_\alpha^2$, the normalized eigenvector of M_2 has exact dynamical-matrix normal-mode weights

$$w_{c,\alpha} = \left(1 + \frac{A_1}{(X_\alpha - \omega_1^2)^2} + \frac{A_2}{(X_\alpha - \omega_2^2)^2}\right)^{-1}, \qquad w_{j,\alpha} = \frac{A_j}{(X_\alpha - \omega_j^2)^2} w_{c,\alpha}, \tag{12}$$

where $A_j := 4\omega_c\omega_j g_j^2 > 0$. By orthogonality of the eigenbasis of symmetric M_2, both row and column sums equal unity identically: $w_{c,\alpha} + w_{1,\alpha} + w_{2,\alpha} = 1$ and $\sum_\alpha w_{k,\alpha} = 1$ (verified to $< 10^{-4}$ across all 9 spectral certificates `C01--C09`).

Theorem 3 (Universal USC Suppression Ceiling on MP^0 Photonic Weight; Lean Thm. 11)**.** *Writing $\Delta_2 := \omega_2^2 - \omega_1^2 > 0$, the Middle Polariton photonic weight obeys the root-free universal upper bound*

$$w_{c,\mathrm{MP}} < \left(1 + \frac{3\min(A_1, A_2) + A_1 + A_2}{\Delta_2^2}\right)^{-1}. \tag{13}$$

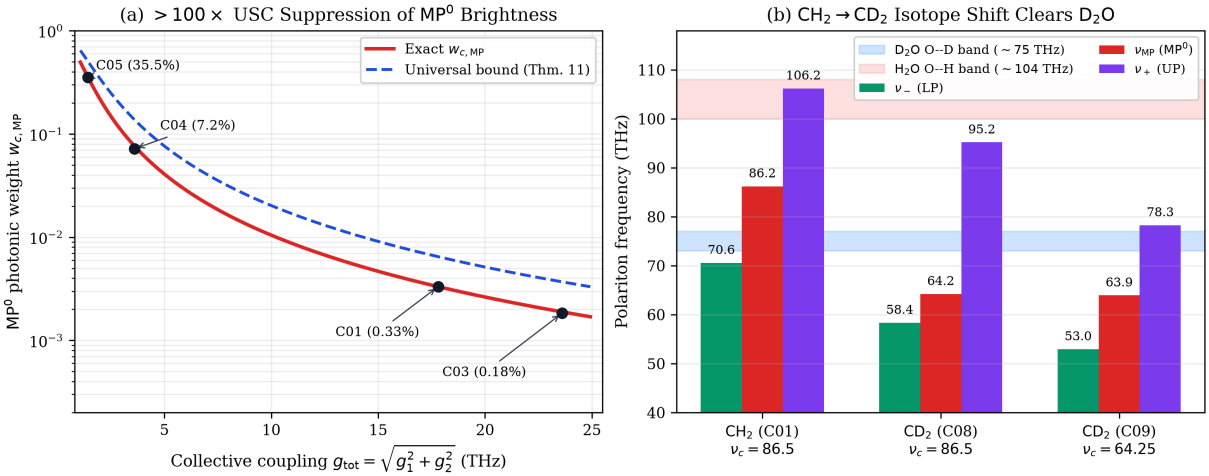

Figure 2: (a) Exact MP^0 photonic weight $w_{c,\mathrm{MP}}$ vs. collective coupling g_{tot} and the root-free universal ceiling of Theorem 3, quantifying the $> 100\times$ brightness suppression from crossover (`C05`) to 71 THz USC (`C01`). (b) Certified $CH_2 \to CD_2$ acyl-chain deuteration shifts (`C08`, `C09`) relative to the D_2O O–D (~ 75 THz) and H_2O O–H (~ 104 THz) solvent absorption bands.

Proof. Set $x = X_{\mathrm{MP}} - \omega_1^2 > 0$ and $y = \omega_2^2 - X_{\mathrm{MP}} > 0$, so $x+y = \Delta_2$. Necessarily $\min(x,y) \le \Delta_2/2$ and $\max(x,y) < \Delta_2$. If $x \le y$, then $4x^2 \le \Delta_2^2$ and $y^2 < \Delta_2^2$, yielding $A_1/x^2 + A_2/y^2 > (4A_1 + A_2)/\Delta_2^2 \ge (3\min(A_1,A_2) + A_1 + A_2)/\Delta_2^2$; the case $y < x$ is symmetric. Inverting yields Eq. (13). □

Physically, Eq. (13) reveals a striking spectroscopic inversion (Fig. 2a). In the moderate strong-coupling regime ($g_1 = 1, g_2 = 1$ THz, `C05`), MP^0 carries 35.48% photonic character and appears as a bright central absorption peak. As collective coupling enters the 71 THz USC regime (`C01`: $g_1 = 11, g_2 = 14$ THz), the cavity repels LP and UP by $\sim$ 16–20 THz while squeezing MP^0 into an almost pure symmetric–antisymmetric matter supermode with $w_{c,\mathrm{MP}} = 0.003318$ (0.33%, strictly below the universal ceiling 0.647%; Lean Thm. 19)—a $> 100\times$ brightness suppression relative to `C05`. Thus, failure to see a bright linear IR peak at 86.2 THz does *not* by itself exclude USC, whereas observing a bright central peak at 86.2 THz quantitatively constrains g_{tot} below USC.

A second clean falsification lever is selective **acyl-chain lipid deuteration** ($CH_2 \to CD_2$, `C08--C09`), which shifts the bare symmetric and antisymmetric stretches to $\nu_1^{(\mathrm{D})} = 62.7$ THz (2091 cm^{-1}) and $\nu_2^{(\mathrm{D})} = 65.8$ THz (2195 cm^{-1}) [6] while scaling the squared dipole couplings by reduced mass $g_j^{(\mathrm{D})2} \approx g_j^2/2$ ($g_1^{(\mathrm{D})} = 7.8$, $g_2^{(\mathrm{D})} = 9.9$ THz). Even in the *unchanged* 86.5 THz cavity (`C08`), exact cubic bracketing (Lean Thm. 18) places the deuterated polariton triplet at

$$\nu_-^{(\mathrm{D})} = 58.3597 \text{ THz}, \qquad \nu_{\mathrm{MP}}^{(\mathrm{D})} = 64.2364 \text{ THz}, \qquad \nu_+^{(\mathrm{D})} = 95.1950 \text{ THz}. \tag{14}$$

Crucially, both $\nu_-^{(\mathrm{D})}$ and $\nu_{\mathrm{MP}}^{(\mathrm{D})}$ shift > 10 THz below the 75 THz D_2O O–D solvent stretch band (Fig. 2b), resolving the aqueous D_2O spectral overlap identified in Wave M1 [4]. If biological modulation tracks the lipid polariton rather than an extraneous cavity or solvent resonance, feeding perdeuterated fatty acids must abolish the 71 THz response and re-emerge near 58.4 THz (or 53.0 THz if the cavity retunes with bilayer index, `C09`).

4 $1/N$ 2D-IR Anharmonicity Discriminator and Dark-Manifold Leakage

4.1 Exact $1/N$ Collective Kerr Suppression

Each individual lipid CH_2 bond carries an intramolecular mechanical anharmonicity $-\frac{1}{2}\hbar\Delta_j(b^\dagger_{j,m})^2 b^2_{j,m}$ with bare values $\Delta_1 \approx 3.6$ THz (120 cm^{-1}) and $\Delta_2 \approx 4.2$ THz (140 cm^{-1}) [9]. Projecting onto the collective bright modes $B_j = N_j^{-1/2}\sum_{m=1}^{N_j} b_{j,m}$ attenuates the polariton Kerr shifts by exact $1/N_j$ factors [10, 13]:

$$\Delta_{\alpha\alpha} = \frac{w_{1,\alpha}^2\Delta_1}{N_1} + \frac{w_{2,\alpha}^2\Delta_2}{N_2}, \qquad \Delta_{\alpha\beta} = 2\left(\frac{w_{1,\alpha}w_{1,\beta}\Delta_1}{N_1} + \frac{w_{2,\alpha}w_{2,\beta}\Delta_2}{N_2}\right) \quad (\alpha \neq \beta). \tag{15}$$

(We note explicitly that retaining full USC Bogoliubov counter-rotating renormalization multiplies the q_j^4 quartic matrix element by $(\omega_j/\nu_\alpha)^2 \approx (86.5/70.6)^2 \approx 1.50$, an $O(1)$ prefactor that leaves the $1/N$ scaling and six-order-of-magnitude collective-vs.-local separation completely intact.)

Theorem 4 (Exact $1/N$ Anharmonicity Bound; Lean Thm. 12)**.** *For any branch α with non-negative normalized weights $w_{1,\alpha} + w_{2,\alpha} \leq 1$, oscillator counts $N_1, N_2 \geq N_{\min} \geq 1$, and bare anharmonicities $0 \leq \Delta_1, \Delta_2 \leq \Delta_{\max}$,*

$$\Delta_{\alpha\alpha} \leq \frac{\Delta_{\max}}{N_{\min}}. \tag{16}$$

As certified in `C10--C12` (Fig. 3a), a crista-scale collective ensemble ($N_1 = N_2 = 10^6$, `C10`) suppresses the 71 THz LP diagonal anharmonicity to $\Delta_{--} = 7.21\times10^{-7}$ THz—$5.82\times10^6\times$ below bare Δ_2 and $> 4\times10^5\times$ below a 0.3 THz homogeneous linewidth. By contrast, a local $N = 1$ defect, impurity, or single-molecule resonance (`C12`) retains $\Delta_{--} = 0.721$ THz (~ 24 cm^{-1}), immediately resolvable as a shifted excited-state absorption (ESA) doublet in diagonal 2D-IR. Furthermore, in collective USC, the $(N_1 + N_2 - 2) = 1{,}999{,}998$ dark modes [10, 14] produce a characteristic **polariton–dark cross-peak and Rabi-contraction bleach** at $(\nu_{\text{pump}}, \nu_{\text{probe}}) = (71, 86.2\text{–}87.5)$ THz, which is strictly absent in a passive dielectric filter or thermal artifact.

4.2 Non-Markovian Dark-Manifold Support Leakage: LP Protection vs. MP^0 Washout

Coupling $N_1 + N_2$ lipid oscillators to one cavity mode via two bright superpositions leaves exactly $(N_1 - 1) + (N_2 - 1) = N_1 + N_2 - 2$ strictly dark eigenstates at ω_1 and ω_2 (Lean Thm. 13). Static inhomogeneous frequency disorder $\delta\omega_{j,m}$ of root-mean-square width σ_{inh} couples each bright mode B_j to its orthogonal dark subspace with exact Hilbert–Schmidt norm $\|V_{B_j\to D_j}\|_2 = \sigma_{\text{inh}}$. For a polariton branch separated from the nearest dark continuum by detuning gap $\delta_{\text{gap}} > 0$, second-order Schur-complement perturbation bounds the dark-manifold leakage probability by [12]

$$\eta_{\text{leak}} \leq \frac{\sigma_{\text{inh}}^2}{\delta_{\text{gap}}^2} \tag{17}$$

(monotonicity machine-checked in Lean Thm. 14). Evaluating Eq. (17) exposes an acute asymmetry between LP and MP^0 (Lean Thm. 15; Fig. 3b):

- **LP Polaron Protection (`C13`):** At $\nu_- \approx 71.0$ THz, $\delta_{\text{gap}} = 85.4 - 71.0 = 14.4$ THz. Even under physiological fluid-bilayer disorder $\sigma_{\text{inh}} = 0.6$ THz (~ 20 cm^{-1}), $\eta_{\text{leak}}(\text{LP}) \leq (0.6/14.4)^2 = 1/576 \approx 0.174\% < 1\%$. The lower polariton is strongly protected against inhomogeneous broadening.

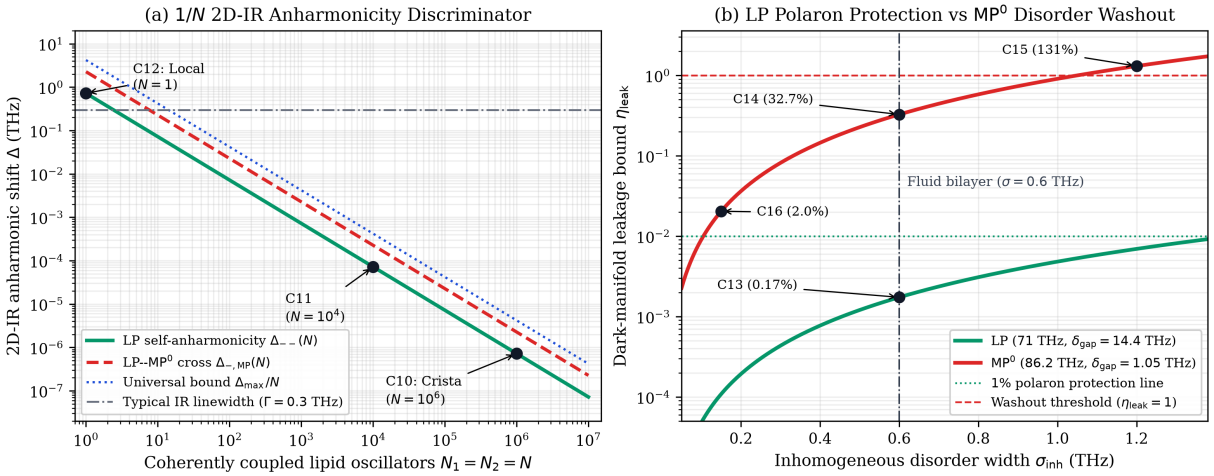

Figure 3: (a) $1/N$ 2D-IR diagonal and cross-anharmonicity discriminator separating a collective crista polariton (`C10`, $N = 10^6$) by six orders of magnitude from a local artifact (`C12`, $N = 1$). (b) Non-Markovian inhomogeneous dark-manifold leakage bound $\eta_{\text{leak}} \leq (\sigma_{\text{inh}}/\delta_{\text{gap}})^2$, contrasting $> 188\times$ stronger polaron protection of LP (`C13`, 0.17%) against MP^0 mixing in fluid bilayers (`C14`, 32.7%) and clean resolution in ordered/gel-phase bilayers (`C16`, 2.0%).

Table 1: Selected exact-$\mathbb{Q}$ certificates from `MITO-TWOBAND-CUBIC-HOPFIELD-CERT-1.0` (`C01--C16`; full SHA-256 manifest in `certificates/MANIFEST.json`).

Cert	Regime / Protocol	ν_- (THz)	ν_{MP} (THz)	ν_+ (THz)	Key Certified Bound
`C01`	Canonical CH_2 USC $(11, 14)$	70.5822	86.2206	106.2124	$w_{c,\text{MP}} = 0.332\%$ (UB 0.647%)
`C02`	Asymmetric CH_2 $(9, 15.4)$	70.7147	85.9507	106.3461	$w_{c,\text{MP}} = 0.271\%$ (UB 0.781%)
`C03`	Deep USC $(14, 19)$	66.1812	86.1571	113.3589	$w_{c,\text{MP}} = 0.183\%$, $\Delta\nu_{\text{ZPE}} = 6.297$
`C04`	Moderate SC $(2, 3)$	82.9930	86.0934	90.4629	$w_{c,\text{MP}} = 7.18\%$ (IR bright)
`C05`	Crossover $(1, 1)$	84.7094	86.4800	88.2335	$w_{c,\text{MP}} = 35.48\%$ ($> 100\times$ `C01`)
`C08`	CD_2, same cavity	58.3597	64.2364	95.1950	> 10 THz below 75 THz D_2O
`C09`	CD_2, retuned 64.25	52.9535	63.9452	78.2821	$\Delta\nu_{\text{ZPE}} = 2.431$ THz
`C10`	2D-IR collective (10^6)	$\Delta_{--} = 7.21 \times 10^{-7}$, $\Delta_{-,\text{MP}} = 2.26 \times 10^{-6}$ THz			$5.82 \times 10^6\times$ suppressed
`C12`	2D-IR local ($N = 1$)	$\Delta_{--} = 0.721$, $\Delta_{-,\text{MP}} = 2.265$ THz			$O(1)$ THz ESA doublet
`C13`	LP leakage ($\sigma = 0.6$)	$\delta_{\text{gap}} = 14.4$ THz, $\eta_{\text{leak}} \leq 1/576$			0.174% (protected)
`C14`	MP^0 fluid ($\sigma = 0.6$)	$\delta_{\text{gap}} = 1.05$ THz, $\eta_{\text{leak}} \leq 16/49$			32.65% ($> 188\times$ LP)
`C16`	MP^0 gel ($\sigma = 0.15$)	$\delta_{\text{gap}} = 1.05$ THz, $\eta_{\text{leak}} \leq 1/49$			2.04% (resolvable)

- MP^0 **Fluid-Bilayer Mixing and Washout (`C14--C15`):** Because MP^0 is trapped inside the 2.1 THz doublet, its maximum possible gap is $\delta_{\text{gap}} \leq 1.05$ THz. At $\sigma_{\text{inh}} = 0.6$ THz, $\eta_{\text{leak}}(\text{MP}^0) \leq 16/49 \approx 32.65\%$ ($> 188\times$ larger than LP), and above $\sigma_{\text{inh}} = 1.05$ THz (`C15`, $\sigma_{\text{inh}} = 1.2$ THz, $\eta_{\text{leak}} = 1.306$) MP^0 washes completely into the dark reservoir.
- **Ordered/Gel-Phase Resolution Window (`C16`):** Cooling or stiffening model membranes into the ordered gel phase narrows CH_2 inhomogeneous disorder to $\sigma_{\text{inh}} \approx 0.15$ THz (~ 5 cm^{-1}) [6], dropping $\eta_{\text{leak}}(\text{MP}^0)$ to $1/49 \approx 2.04\%$ and reopening a sharp Raman/2D-IR visibility window for MP^0.

5 Verification Boundary, Spectroscopic Caveats, and Experimental Matrix

To preserve strict epistemic transparency, we separate our claims into three explicit layers:

1. **Lean 4.36.0 Kernel Layer (Machine-Checked):** All 20 theorems in `MitoTwoBandCubicHopfieldCert.lean` compile under `lean -DwarningAsError=true` and `lake build` with 0 `sorry`, 0 `grind`, and 0 `Classical.choice` (audited via `#print axioms`; only constructive `propext`/`Quot.sound` or zero axioms). This layer proves the exact TRK cubic factorization, global stability on $(-\infty, 0]$, strict Cauchy–Hopfield pivot signs, the calculus-free AM–GM proof of universal two-band ZPE positivity, the root-free universal MP^0 photonic suppression inequality, the $1/N$ anharmonicity bound, dark-manifold dimensionality, leakage monotonicity, and exact integer-scaled root brackets for `C01`, `C02`, and `C08`.

2. **Exact-$\mathbb{Q}$ Python Certificate Layer:** The exact rational verifier module (`src/mito_twoband_cubic_hopfield_verifier.py`) is AST-audited to contain zero floats, zero `/` or `**` operators, and zero `limit_denominator` calls. It certifies 16 canonical JSON records (`C01--C16`, SHA-256 locked in `MANIFEST.json`) and passes 57/57 adversarial `pytest` checks.

3. **Physical Modeling Caveats and Unverified Experimental Hypotheses:** Real fluid phospholipid membranes exhibit weak Fermi-resonance mixing between the CH_2 symmetric stretch (~ 2850 cm^{-1}) and the CH_2 scissoring overtone $2\delta(CH_2)$ (~ 2890 cm^{-1}) [5, 6], as well as terminal CH_3 stretches ($\sim 2872/2960$ cm^{-1}); extending the secular polynomial to K vibrational bands preserves exact TRK Cauchy interlacing with $K-1$ trapped middle polaritons. Moreover, our 71 THz couplings (g_1, g_2) are conditioned on the unrefereed empirical claim of Ref. [1]; whether intact cristae actually achieve subwavelength cavity confinement and USC oscillator strength remains unverified [4].

Together, our theorems prescribe a decisive three-experiment falsification protocol: (i) 2D-IR diagonal anharmonicity at 71 THz ($\Delta_{--} < 10^{-5}$ THz with $(71, 86.2\text{–}87.5)$ THz cross-peak for collective USC vs. $\Delta_{--} \sim 0.7$ THz for a local mode); (ii) ordered/gel-phase Raman or 2D-IR search for the trapped MP^0 near 86.0–86.2 THz ($\eta_{\mathrm{leak}} \leq 2\%$ at $\sigma_{\mathrm{inh}} = 0.15$ THz); and (iii) acyl-chain $CH_2 \to CD_2$ deuteration shifting LP and MP^0 cleanly to 58.4 and 64.2 THz, free of D_2O solvent interference.

References

[1] Y. Yang, H. Gu, and B. Song. Mitochondrial cristae as mid-infrared polaritonic cavities modulating cellular atp synthesis. Unrefereed preprint, bioRxiv:10.64898/2026.09.10.750628v1, September 2026. Unrefereed preprint awaiting independent experimental replication.

[2] Lluis Eriksson. Geometry and resource boundaries for biological polariton models. AIRR.SCIENCE Record ARR-2025-2AQXS44H6Z8GQAG2, 2025.

[3] Lluis Eriksson. Mito-polariton resource-boundary certificates and exact thermodynamic audits. AIRR.SCIENCE Record ARR-2026-1E91AXEJYT890TQC, 2026.

[4] Lluis Eriksson. Mitochondrial polariton audit series wave m1: Subwavelength confinement, dressed usc thermodynamics, and atp modulation bounds. AIRR.SCIENCE Records ARR-2026-75841S47Z59VMSN2, ARR-2026-038Y5T8GYG9F7TTR, and ARR-2026-0CXEJ0MRT995CAK8, 2026.

[5] R. G. Snyder, S. L. Hsu, and S. Krimm. Vibrational spectra in the c–h stretching region and the structure of the polymethylene chain. *Spectrochimica Acta Part A: Molecular Spectroscopy*, 34(4):395–406, 1978.

[6] Henry H. Mantsch and Ronald N. McElhaney. Phospholipid phase transitions in model and biological membranes as studied by infrared spectroscopy. *Chemistry and Physics of Lipids*, 57(2–3):213–226, 1991.

[7] J. J. Hopfield. Theory of the contribution of excitons to the complex dielectric constant of crystals. *Physical Review*, 112(5):1555–1567, 1958.

[8] Anton Frisk Kockum, Adam Miranowicz, Simone De Liberato, Salvatore Savasta, and Franco Nori. Ultrastrong coupling between light and matter. *Nature Reviews Physics*, 1:19–40, 2019.

[9] Peter Hamm and Martin Zanni. *Concepts and Methods of 2D Infrared Spectroscopy*. Cambridge University Press, 2011.

[10] Bo Xiang, Raphael F. Ribeiro, Adam D. Dunkelberger, Jiaxi Wang, Yingmin Li, Blake S. Simpkins, Jeffrey C. Owrutsky, Joel Yuen-Zhou, and Wei Xiong. Two-dimensional infrared spectroscopy of vibrational polaritons. *Proceedings of the National Academy of Sciences*, 115(19):4845–4850, 2018.

[11] Adam D. Dunkelberger, Blake S. Simpkins, Igor Vurgaftman, and Jeffrey C. Owrutsky. Vibration-cavity polariton chemistry and dynamics. *Annual Review of Physical Chemistry*, 73:429–451, 2022.

[12] R. Houdré, R. P. Stanley, and M. Ilegems. Vacuum-field rabi splitting in the presence of inhomogeneous broadening: Resolution of a homogeneous linewidth in an inhomogeneously broadened system. *Physical Review A*, 53(4):2711–2715, 1996.

[13] Raphael F. Ribeiro, Luis A. Martínez-Martínez, Matthew Du, Jorge Campos-Gonzalez-Angulo, and Joel Yuen-Zhou. Polariton chemistry: controlling molecular dynamics with optical cavities. *Chemical Science*, 9(30):6325–6339, 2018.

[14] Bo Xiang, Raphael F. Ribeiro, Matthew Du, Liying Chen, Zimo Yang, Jiaxi Wang, Joel Yuen-Zhou, and Wei Xiong. Intermolecular vibrational energy transfer enabled by microcavity strong light-matter coupling. *Science*, 368(6491):665–667, 2020.